Nucleus Journal
Jurnal Sains dan Teknologi
Website: https://ejournal.undar.or.id/index.php/Nucleus
e-ISSN: 2964-4100
p-ISSN: 2964-4097

Catalytic Pyrolysis of Polypropylene Using Nickel Supported Sago Waste Activated Carbon for Liquid Fuel

[1]Syukrika Putri, [2*]Nurmalasari, [3]Suci Ramadani, [4]Dian Safitri
[1,2,3,4] Metallurgical Engineering Study Program, Institut Teknologi Bacharuddin Jusuf Habibie, Parepare, Indonesia
[1]syukrikaputri@ith.ac.id, [2]nurmalasari@ith.ac.id, [3]suci.mahasiswa@ith.ac.id, [4]dian.mahasiswa@ith.ac.id

Article Info

Article history:

Received: 8 March 2026
Revised: 1 April 2026
Accepted: 27 April 2026

Keyword:

catalytic
polypropylene
nickel catalyst
activated carbon
liquid hydrocarbons

ABSTRACT

The catalytic pyrolysis of polypropylene (PP) has attracted significant attention as a promising route for converting plastic waste into valuable fuels; however, the development of low-cost and sustainable catalysts remains a major challenge. While Ni-based catalysts have been widely studied, the use of biomass-derived activated carbon, particularly from sago waste, as a support material and the systematic evaluation of catalyst-to-plastic ratio on hydrocarbon selectivity remain insufficiently explored. In this study, catalytic pyrolysis of polypropylene was performed at 500 °C using Ni supported on activated carbon (Ni/AC) derived from sago waste, with catalyst amounts of 2.5, 5.0, and 7.5 g, alongside a non-catalytic run for comparison. The introduction of Ni/AC substantially increased liquid yield compared to thermal pyrolysis, with the highest yield (39.75%) obtained at 2.5 g. Increasing catalyst amount intensified secondary cracking reactions, leading to enhanced gas formation at the expense of liquid products. GC–MS analysis revealed that the liquid products were mainly composed of hydrocarbons in the gasoline (C5–C12) and diesel (C13–C20) ranges. These results highlight the critical role of catalyst loading in controlling product distribution and hydrocarbon selectivity. This study demonstrates the potential of sago waste-derived Ni/AC as a sustainable catalyst and provides new insight into the relationship between catalyst amount and hydrocarbon selectivity in catalytic pyrolysis systems.

DOI: https://doi.org/10.32492/nucleus.v5i1.5102

Corresponding Author:
Nurmalasari
Metallurgical Engineering Study Program, Institut Teknologi Bacharuddin Jusuf Habibie
Parepare, Sulawesi Selatan, Indonesia
Email: nurmalasari@ith.ac.id

I. INTRODUCTION

Plastic consumption has increased significantly in recent decades due to rapid industrialization and population growth, resulting in the accumulation of persistent plastic waste in the environment. In 2021, global plastic production exceeded 390 million tons and is projected to continue increasing, posing serious environmental challenges due to the high resistance of plastics to natural degradation [1], [2], [3]. In Indonesia, plastic waste constitutes a major fraction of municipal solid

waste, exceeding 10 million tons annually and continuing to rise [4]. This condition highlights the urgent need for sustainable technologies that not only reduce plastic waste but also recover valuable products.

Among various polymers, polypropylene (PP) is widely used in packaging and consumer products due to its favorable mechanical and chemical properties. However, its extensive use has led to significant post-consumer waste accumulation. Pyrolysis has emerged as a promising approach for converting plastic waste into fuels and chemicals, reducing waste volume while producing liquid hydrocarbons, gases, and solid residues [5], [6], [7], [8]. Despite these advantages, non-catalytic pyrolysis often results in low product selectivity and a broad distribution of hydrocarbons, limiting the direct applicability of the liquid products as fuels [9], [10], [11].

To address these limitations, catalytic pyrolysis has been extensively investigated as an effective approach to enhance product selectivity and promote the formation of desirable fuel-range hydrocarbons [11], [12], [13]. Among various catalysts, nickel-based catalysts have attracted considerable attention due to their ability to facilitate cracking and hydrogen transfer reactions at relatively moderate temperatures, offering a cost-effective alternative to noble metals [14], [15], [16]. However, Ni catalysts are prone to deactivation through sintering and agglomeration under high-temperature conditions, necessitating the use of suitable supports to enhance metal dispersion, structural stability, and overall catalytic performance [17].

Activated carbon has been widely recognized as a promising catalyst support due to its high surface area, tunable pore structure, and strong metal–support interactions, which promote effective metal dispersion and catalytic activity [18], [19], [20], [21].

Recent studies have investigated Ni-based catalysts supported on various materials such as zeolites, alumina, and conventional activated carbon for polypropylene pyrolysis, demonstrating enhanced cracking activity and improved hydrocarbon selectivity. Ni-supported zeolites, for instance, are known to promote gasoline-range hydrocarbons due to their strong acidity [16], [22], while Ni supported on alumina offers good thermal stability but often results in relatively lower liquid selectivity [23]. In contrast, porous carbon supports offer high surface area and improved metal dispersion, which can enhance catalytic performance while suppressing coke formation.

However, these studies predominantly rely on conventional or commercially available supports, with limited integration of sustainable biomass-derived materials. In addition, although catalyst loading has been reported to influence product distribution through secondary cracking reactions, most investigations focus on traditional catalyst systems. Systematic studies that simultaneously evaluate biomass-derived carbon supports and catalyst-to-plastic ratio remain scarce, particularly in understanding how catalyst amount governs the balance between liquid yield, gas formation, and coke suppression.

One promising yet underexplored biomass resource within this context is sago waste, a by-product of starch processing. Activated carbon derived from sago waste has demonstrated promising physicochemical properties for catalytic applications. Despite these advantages, its application as a catalyst support in plastic pyrolysis has not been systematically investigated, especially in relation to the interaction between Ni loading and product selectivity.

Despite these advances, the performance of Ni-based catalysts in plastic pyrolysis remains strongly influenced by catalyst loading and support characteristics, particularly when biomass-derived carbon materials are used. The mechanistic role of catalyst-to-plastic ratio in controlling reaction pathways, product distribution, and hydrocarbon selectivity remains insufficiently understood.

Therefore, this study aims to address these gaps by investigating the catalytic pyrolysis of polypropylene using Ni supported on activated carbon derived from sago waste, with a particular focus on the mechanistic role of catalyst loading. This work provides a systematic evaluation of how catalyst-to-plastic ratio governs the transition between primary cracking and secondary

reactions, thereby controlling liquid yield, hydrocarbon selectivity toward gasoline- and diesel-range products, and coke formation. By integrating sustainable material development with mechanistic insights, this study demonstrates that catalyst loading is not merely an operational variable, but a fundamental parameter governing the transition between primary cracking, secondary reactions, and overcracking pathways in biomass-derived Ni/AC systems.

II. METHODS

A. Materials

Polypropylene (PP) used as feedstock was obtained from commercial plastic packaging waste and cut into small particles of approximately 1–3 mm prior to use. Sago waste biomass was collected from a local sago processing facility located in Luwu Regency, South Sulawesi, Indonesia, and utilized as a precursor for activated carbon production. Nickel nitrate hexahydrate ($Ni(NO_3)_2 \cdot 6H_2O$, Merck) was used as the nickel precursor for catalyst preparation. Potassium hydroxide (KOH, Merck) was employed as a chemical activating agent. All chemicals were of analytical grade and used without further purification. Nitrogen gas (N_2) was employed to provide an inert atmosphere during all thermal processes.

B. Preparation of Activated Carbon from Sago Waste

Activated carbon was prepared from sago waste via carbonization followed by KOH-assisted chemical activation. The raw biomass was thoroughly washed with distilled water and dried at 105 °C for 24 h. Carbonization was carried out in a tubular furnace at 500 °C under a nitrogen flow of 100 mL/min with a heating rate of 10 °C/min to obtain char.

The resulting char was chemically impregnated with potassium hydroxide (KOH) at an impregnation ratio of 1:1 (char:KOH, w/w). The impregnation process was conducted at 90 °C for 12 h under reflux conditions to promote interaction between the activating agent and the carbon matrix. The impregnated sample was then dried at 105 °C for 2 h.

Thermal activation was subsequently performed at 500 °C for 2 h under nitrogen flow (100 mL/min) with a heating rate of 10 °C/min to develop the pore structure. After activation, the sample was washed repeatedly with distilled water until neutral pH was achieved to remove residual activating agents and soluble by-products. The activated carbon was dried at 105 °C for 12 h and stored in a desiccator prior to catalyst preparation.

C. Preparation of Ni/AC Catalyst

Ni-supported activated carbon (Ni/AC) catalysts were prepared using the wet impregnation method with a target nickel loading of 1 wt%. A calculated amount of $Ni(NO_3)_2 \cdot 6H_2O$ corresponding to a target loading of 1 wt% Ni relative to the mass of activated carbon was dissolved in 50 mL of distilled water. The solution was added dropwise to the activated carbon under continuous stirring to ensure homogeneous distribution of the nickel precursor. The mixture was stirred for 4 h at room temperature without an additional aging step.

The impregnation was performed under ambient conditions. The impregnated sample was dried at 100 °C for 12 h to remove moisture. Calcination was then carried out at 500 °C for 2 h under a nitrogen atmosphere (20 mL/min) with a heating rate of 5 °C/min. The resulting catalyst was cooled to room temperature under nitrogen flow and stored in airtight containers for further use.

D. Catalyst Characterization

The textural properties of the activated carbon and Ni/AC catalysts were analyzed using N_2 adsorption–desorption measurements. The specific surface area was calculated using the Brunauer–Emmett–Teller (BET) method. Surface morphology and elemental composition were examined using scanning electron microscopy (SEM).

E. Catalytic Pyrolysis

Catalytic pyrolysis experiments were conducted in a laboratory-scale fixed-bed batch reactor made of stainless steel with an internal volume of 20 mL. In each run, 10 g of polypropylene feedstock (particle size 1–3 mm) was thoroughly mixed with the catalyst to ensure homogeneous contact.

Catalyst-to-plastic ratios of 0.25, 0.50, and 0.75 (w/w) were applied, corresponding to catalyst masses of 2.5 g, 5.0 g, and 7.5 g, respectively.

Prior to heating, the reactor was purged with nitrogen to remove residual air. The system was then heated to 500 °C under a continuous nitrogen flow of 25 mL/min and maintained at this temperature for 60 min. The experiment was conducted under a fixed-bed configuration without mechanical agitation; therefore, vapor–solid interactions were governed by diffusion and contact time within the packed bed.

The resulting vapors were passed through a water-cooled condenser (~10 °C) for liquid collection. Non-condensable gases were not directly quantified and were released from the system. A non-catalytic experiment was performed under identical conditions for comparison. All experiments were conducted in triplicate, and the reported values represent mean results.

F. Product Analysis

The yields of liquid and solid products were determined gravimetrically. The liquid fraction collected in the condenser was weighed directly, while the solid residue remaining in the reactor was quantified as char or coke. The gas yield was calculated by difference based on mass balance.

The overall mass balance closure ranged between 95–100%, indicating acceptable experimental consistency. While gas products were not compositionally analyzed, this approach provides a reasonable basis for comparative evaluation across different experimental conditions, although detailed gas composition analysis would be required for a more comprehensive understanding of reaction pathways.

All experimental data are presented as mean values from triplicate runs, with deviations of less than 5%, indicating good reproducibility. The chemical composition of liquid products was analyzed using Gas Chromatography–Mass Spectrometry (GC–MS, Shimadzu QP2010). Identified compounds were classified into hydrocarbon groups based on carbon number distribution: gasoline-range (C5–C12) and diesel-range (C13–C20).

III. Results and Discussion

A. Textural and Morphological Properties of Ni/AC Catalyst

The textural and morphological properties of the Ni/AC catalyst were investigated to understand the structural characteristics that influence its catalytic performance during polypropylene pyrolysis. The BET analysis revealed that the prepared catalyst possessed a surface area of 134 m^2/g, indicating the presence of a sufficiently developed porous structure that can facilitate adsorption and catalytic reactions.

Further insight into the pore structure was obtained from nitrogen adsorption–desorption analysis. The isotherm shown in Figure 1 exhibits a gradual increase in adsorption volume over the entire relative pressure range, along with a noticeable hysteresis loop at higher P/Po values. This behavior suggests the coexistence of microporous and mesoporous structures, corresponding to a Type IV isotherm with microporous contributions. Such features are typically associated with interconnected pore networks and “ink-bottle”-type mesopores that enhance diffusion within the material.

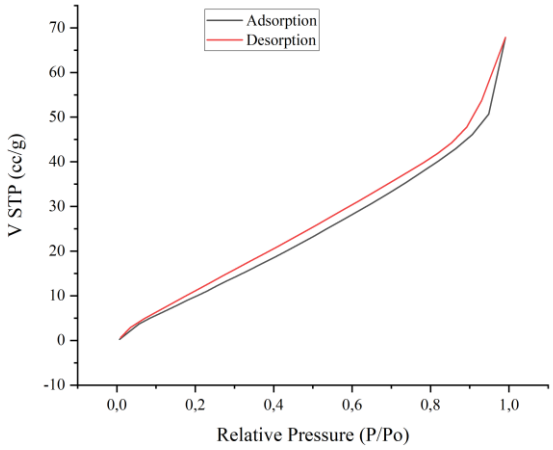

Figure 1. Adsorption–desorption isotherm of Ni/AC catalyst

The pore size distribution analysis (Figure 2) reveals a dominant pore radius centered at approximately 13.7 Å (1.37 nm), confirming that the catalyst is predominantly microporous with secondary mesoporous features. In addition, the presence of a distribution tail extending toward larger pore sizes (up to ~30 Å) indicates the existence of small mesopores. This confirms that the Ni/AC catalyst possesses a hierarchical pore structure consisting of micropores and mesopores.

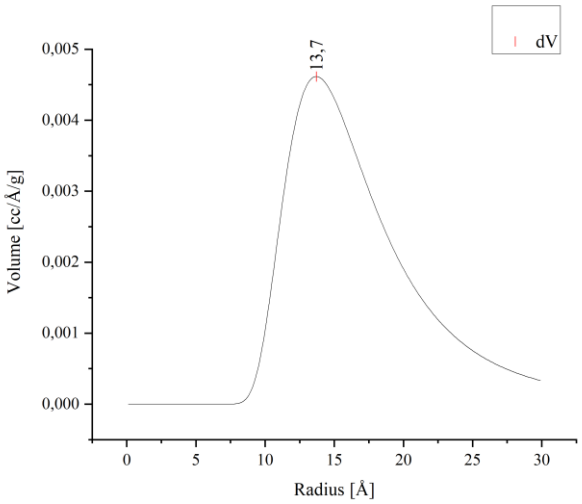

Figure 2. Pore size distribution of Ni/AC catalyst

This pore size distribution is consistent with the adsorption–desorption isotherm behavior observed in Figure 1. The presence of a hysteresis loop at high relative pressure (P/Po > 0.8) indicates capillary condensation within mesopores, while the continuous adsorption at low relative pressure suggests the contribution of micropore filling. The dominant pore radius (~1.37 nm) confirms that the pore system is primarily microporous, whereas the extended distribution toward larger pore sizes reflects the presence of secondary mesopores. This combination explains the Type IV isotherm with microporous characteristics, where micropores govern adsorption capacity and mesopores contribute to diffusion pathways. Such structural features are particularly important in catalytic pyrolysis, as they facilitate the transport of bulky polypropylene-derived intermediates while maintaining sufficient active surface for cracking reactions [24], [25].

The coexistence of micropores and mesopores plays a critical role in catalytic performance. Micropores contribute to high adsorption capacity and provide abundant active sites for the initial

cracking of hydrocarbon intermediates, while mesopores facilitate the diffusion of larger polymer-derived molecules into the internal structure of the catalyst. This dual-porosity system has been widely recognized as a critical factor in improving catalytic efficiency in gas–solid reactions, as it enables both effective adsorption and enhanced mass transport within the catalyst structure [24], [25], [26], [27].

Further insights into the catalyst structure were obtained from SEM analysis. As shown in Figure 3, the surface morphology of the Ni/AC catalyst exhibits a rough carbon matrix with irregular cavities and pores. Bright contrast regions observed on the carbon surface are attributed to the presence of nickel particles dispersed on the activated carbon support. The distribution of Ni particles both on the external surface and within larger pores suggests a relatively good metal dispersion.

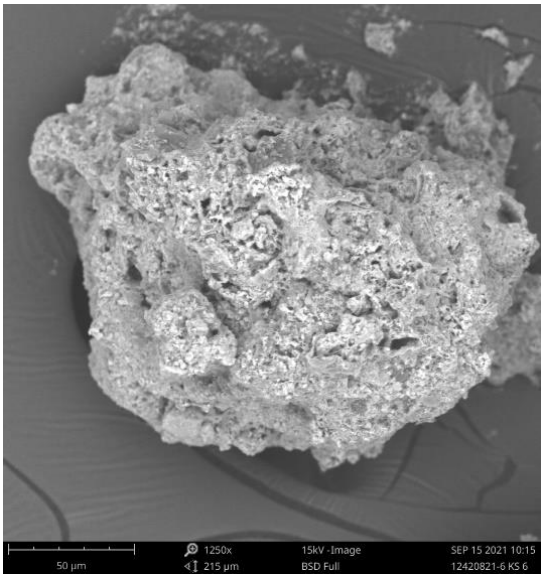

Figure 3. SEM morphology of Ni/AC catalyst

Such dispersion is advantageous for catalytic applications because it provides accessible active sites while maintaining open diffusion pathways within the porous structure. Similar observations have been reported in previous studies on nickel supported porous carbon catalysts, suggesting relatively good dispersion of nanoparticles within hierarchical pore systems significantly enhanced catalytic activity in hydrogenation and reforming reactions while minimizing diffusion limitations [28], [29], [30].

Taken together, the BET and SEM analyses confirm that the prepared Ni/AC catalyst exhibits a hierarchical pore architecture combining microporous and mesoporous. This structural feature is beneficial for catalytic processes, as it simultaneously promotes adsorption capacity, efficient mass transfer, and accessible active sites. Such characteristics are widely recognized as important factors contributing to improved catalytic performance and stability under demanding gas–solid reaction conditions [31], [32].

This hierarchical pore structure is expected to strongly influence the catalytic cracking behavior observed in the following sections, particularly in controlling product distribution and hydrocarbon selectivity.

B. Effect of Catalyst Amount on Product Distribution

The influence of Ni/AC catalyst amount on the distribution of pyrolysis products is summarized in Table 1. In the absence of a catalyst, polypropylene pyrolysis produced only 14% liquid yield, indicating that thermal pyrolysis alone has limited efficiency in converting polymer chains into

condensable hydrocarbons. The introduction of Ni/AC catalyst substantially increased liquid production.

Table 1. Effect of catalyst amount on product distribution

PP: Ni/AC (g)	Liquid Quantity (%)	Gas Quantity (%)	Coke Quantity (%)
100 : 0	14.00	32.00	54
100 : 2.5	39.75	59.00	1.25
100 : 5	32.88	66.00	1.12
100 : 7.5	32.00	67.00	1.00

The highest liquid yield (39.75%) was obtained with a catalyst amount of 2.5 g, which is nearly three times higher than that obtained from non-catalytic pyrolysis. This result indicates that the Ni/AC catalyst effectively promotes the catalytic cracking of long-chain polypropylene into shorter hydrocarbons that readily condense into liquid products [33], [34].

However, increasing the catalyst amount beyond this level resulted in a decrease in liquid yield. At catalyst masses of 5 g and 7.5 g, the liquid yields decreased to 32.88% and 32%, respectively. This reduction can be attributed to enhanced secondary cracking reactions, in which intermediate liquid hydrocarbons are further converted into lighter gaseous products [16], [35].

The gaseous fraction exhibited an inverse trend compared to the liquid yield, increasing from 32% in non-catalytic pyrolysis to 67% at the highest catalyst loading. This behavior confirms that higher catalyst amounts intensify cracking reactions, favoring the formation of lighter gaseous hydrocarbons at the expense of condensable products.

A notable observation is the drastic reduction in coke formation in the presence of the Ni/AC catalyst. While thermal pyrolysis produced 54% coke, the addition of the catalyst reduced this value to approximately 1%. This significant decrease indicates that the catalyst enhances chain scission efficiency and suppresses polymer condensation pathways, thereby minimizing the formation of solid carbon residues [34], [36].

Overall, these results highlight the critical role of catalyst amount in controlling product selectivity during catalytic pyrolysis. An optimal catalyst amount of 2.5 g provides the best balance between maximizing liquid yield and minimizing coke formation. However, liquid yield alone is insufficient to evaluate fuel quality, as the composition of the liquid fraction determines its classification within gasoline- or diesel-range hydrocarbons.

From a mechanistic perspective, the observed behavior can be explained by the interaction between active sites and reaction pathways. At lower catalyst loading (2.5 g), the number of active sites is sufficient to promote primary cracking of polypropylene into condensable hydrocarbons, resulting in the highest liquid yield with limited secondary reactions.

As the catalyst amount increases to 5 g and 7.5 g, the higher density of active sites enhances secondary cracking through β-scission and hydrogen transfer mechanisms [35], [37]. These reactions further decompose intermediate liquid hydrocarbons into lighter gaseous products, leading to a decrease in liquid yield and an increase in gas formation. The shift in hydrocarbon selectivity is also influenced by catalyst loading. At moderate catalyst amount (5 g), the balance between cracking and stabilization favors the formation of longer-chain hydrocarbons, resulting in higher diesel selectivity. In contrast, excessive catalyst loading (7.5 g) promotes overcracking, leading to the formation of shorter-chain hydrocarbons in the gasoline range.

In addition, the suppression of coke formation suggests that the Ni active sites may facilitate hydrogen transfer reactions that stabilize reactive intermediates and inhibit the formation of coke precursors. This highlights the synergistic role of metal sites and the carbon support in directing

reaction pathways. These findings demonstrate that catalyst amount governs the balance between primary and secondary cracking reactions, ultimately determining product distribution, hydrocarbon selectivity, and coke formation during polypropylene pyrolysis.

C. Hydrocarbon Composition of Liquid Products

GC–MS analysis showed that the liquid products obtained from both thermal and catalytic pyrolysis predominantly consisted of hydrocarbons within the gasoline (C5–C12) and diesel (C13–C20) ranges. The distribution of these fractions was significantly influenced by the presence of the Ni/AC catalyst and the catalyst loading.

At lower catalyst loading (2.5 g), the liquid products exhibited a relatively balanced distribution of gasoline- and diesel-range hydrocarbons, corresponding to the highest liquid yield. Increasing the catalyst loading to 5 g resulted in an increased proportion of diesel-range hydrocarbons, indicating enhanced conversion of long-chain intermediates into mid-range fractions. In contrast, at higher catalyst loading (7.5 g), the product distribution shifted toward lighter hydrocarbons, with a higher fraction of gasoline-range compounds accompanied by increased gas formation.

This trend confirms that catalyst loading governs hydrocarbon selectivity through the regulation of secondary cracking intensity, where moderate loading favors diesel-range products, while excessive loading promotes overcracking toward gasoline-range hydrocarbons and gaseous products. The quantitative distribution of hydrocarbon fractions is summarized in Table 2.

Table 2. Distribution of hydrocarbon fractions based on GC–MS analysis

Carbon Range	Ni/AC (0 g)	Ni/AC (2.5 g)	Ni/AC (5 g)	Ni/AC (7.5 g)
C5 C12	67.01	43.78	41.86	77.05
C13 C20	32.57	55.56	58.14	22.95
>C20	0.42	0.66	0	0

The results show that the catalytic system exhibits considerable selectivity toward fuel-range hydrocarbons. The gasoline fraction reached its highest value (77.05%) when 7.5 g of Ni/AC catalyst was used, while the highest diesel fraction (58.14%) was obtained at a catalyst amount of 5 g. These distributions reflect intensified secondary cracking reactions, leading to the formation of shorter hydrocarbon fractions [34], [35].

The major compounds identified in the liquid products were predominantly aliphatic hydrocarbons, including alkanes such as C8H18 and C17H36, as well as alkenes such as C9H18 and C10H20. These compounds are commonly found in commercial gasoline and diesel fuels, indicating that the pyrolysis products possess characteristics like conventional petroleum-derived fuels.

Interestingly, increasing the catalyst amount to 7.5 g resulted in a decrease in the diesel fraction. This observation suggests that excessive catalyst amounts promote additional cracking of heavier hydrocarbons into lighter gasoline-range compounds and gaseous products. Consequently, an excessive catalyst concentration may shift the product distribution toward lighter hydrocarbons, reducing diesel selectivity. These findings demonstrate that catalyst amount plays a critical role in determining hydrocarbon distribution during polypropylene pyrolysis. While 2.5 g of Ni/AC provides the highest liquid yield, higher catalyst amounts can modify hydrocarbon selectivity toward lighter fractions.

This approach provides a potential pathway for converting plastic waste into valuable fuel products. The use of activated carbon derived from sago waste provides an environmentally friendly catalyst support while simultaneously utilizing agricultural biomass residues. Overall, the results confirm that activated carbon derived from sago waste is an effective catalyst support for Ni catalysts, providing a sustainable and low-cost alternative for plastic waste conversion into fuel-like hydrocarbons.

IV. CONCLUSIONS

This study demonstrates that Ni supported on activated carbon derived from sago waste is an effective and sustainable catalyst for the pyrolysis of polypropylene. The catalyst exhibits a hierarchical micro–mesoporous structure with a surface area of 134 m^2/g, enabling efficient adsorption, diffusion, and catalytic transformation of polymer-derived intermediates. The introduction of Ni/AC significantly enhances liquid yield and suppresses coke formation compared to non-catalytic pyrolysis.

More importantly, this work establishes catalyst loading as a critical parameter governing reaction pathways and product distribution. At low catalyst loading, primary cracking dominates, resulting in maximum liquid yield. At moderate loading, the balance between cracking and stabilization favors diesel-range hydrocarbons, while higher loading intensifies secondary cracking, leading to increased gas formation and gasoline-range selectivity. These findings provide clear mechanistic insight into how catalyst loading controls the transition between liquid preservation, selective hydrocarbon production, and overcracking.

By systematically linking catalyst structure, active sites, and reaction behavior, this study advances the understanding of catalytic pyrolysis systems and highlights the potential of biomass-derived activated carbon as a low-cost and environmentally friendly catalyst support. The results demonstrate that the catalytic performance of Ni/AC is governed by the interplay between pore structure and Ni loading. The hierarchical pore distribution facilitates the diffusion and transformation of pyrolysis intermediates, while appropriate Ni loading enhances active site availability without blocking micropores. This synergy leads to improved catalytic efficiency and product selectivity. This study provides new insights into the role of biomass-derived activated carbon as a catalyst support, highlighting the importance of optimizing metal loading to achieve a balance between surface area utilization and catalytic activity in plastic waste conversion.

V. ACKNOWLEDGMENT

The authors gratefully acknowledge the financial support from the Directorate General of Higher Education, Research, and Technology (DPPM Dikti Saintek) through the Penelitian Dosen Pemula (PDP) scheme under contract number 014/C3/DT.05.00/PL/2025. Additional support from Institut Teknologi Bacharuddin Jusuf Habibie under derivative contract number 027/IT13.D/KH DPPM/2025 is also duly acknowledged.

VI. REFERENCES

[1] H. Ritchie, V. Samborska, and M. Roser, "Plastic Pollution," *Our World Data*, Nov. 2023, Accessed: Sep. 22, 2025. [Online]. Available: https://ourworldindata.org/plastic-pollution

[2] K. Ziani *et al.*, "Microplastics: A Real Global Threat for Environment and Food Safety: A State of the Art Review," *Nutrients*, vol. 15, no. 3, p. 617, Jan. 2023, doi: 10.3390/nu15030617.

[3] OECD, *Global Plastics Outlook: Economic Drivers, Environmental Impacts and Policy Options*. OECD, 2022. doi: 10.1787/de747aef-en.

[4] K. L. H. dan Kehutanan, "KLHK Ajak Masyarakat 'Gaya Hidup Minim Sampah' Dalam Festival LIKE 2," KLHK Ajak Masyarakat "Gaya Hidup Minim Sampah" Dalam Festival LIKE 2. Accessed: Sep. 22, 2025. [Online]. Available: https://www.menlhk.go.id/news/klhk-ajak-masyarakat-gaya-hidup-minim-sampah-dalam-festival-like-2

[5] J. Deng *et al.*, "Co-pyrolysis of biomass and plastic waste into carbon materials with environmental applications: a critical review," *Green Chem.*, vol. 27, no. 22, pp. 6320–6341, 2025, doi: 10.1039/D4GC04842C.

[6] M. M. Harussani, S. M. Sapuan, U. Rashid, A. Khalina, and R. A. Ilyas, "Pyrolysis of polypropylene plastic waste into carbonaceous char: Priority of plastic waste management amidst COVID-19 pandemic," *Sci. Total Environ.*, vol. 803, p. 149911, Jan. 2022, doi: 10.1016/j.scitotenv.2021.149911.
[7] H. Yaqoob, H. Muhammad Ali, and U. Khalid, "Pyrolysis of waste plastics for alternative fuel: a review of key factors," *RSC Sustain.*, vol. 3, no. 1, pp. 208–218, 2025, doi: 10.1039/D4SU00504J.
[8] Z. Shareefdeen and A. T. ElGazar, "Management of Plastic Wastes through Recent Advanced Pyrolysis Processes," *Appl. Sci.*, vol. 14, no. 14, p. 6156, Jan. 2024, doi: 10.3390/app14146156.
[9] T. Maqsood, J. Dai, Y. Zhang, M. Guang, and B. Li, "Pyrolysis of plastic species: A review of resources and products," *J. Anal. Appl. Pyrolysis*, vol. 159, p. 105295, Oct. 2021, doi: 10.1016/j.jaap.2021.105295.
[10] A. Antelava *et al.*, "Energy Potential of Plastic Waste Valorization: A Short Comparative Assessment of Pyrolysis versus Gasification," *Energy Fuels*, vol. 35, no. 5, pp. 3558–3571, Mar. 2021, doi: 10.1021/acs.energyfuels.0c04017.
[11] N. Javed *et al.*, "Analysis of Fuel Alternative Products Obtained by the Pyrolysis of Diverse Types of Plastic Materials Isolated from a Dumpsite Origin in Pakistan," *Polymers*, vol. 15, no. 1, p. 24, Dec. 2022, doi: 10.3390/polym15010024.
[12] S. D. Anuar Sharuddin, F. Abnisa, W. M. A. Wan Daud, and M. K. Aroua, "A review on pyrolysis of plastic wastes," *Energy Convers. Manag.*, vol. 115, pp. 308–326, May 2016, doi: 10.1016/j.enconman.2016.02.037.
[13] S. M. Al-Salem, A. Antelava, A. Constantinou, G. Manos, and A. Dutta, "A review on thermal and catalytic pyrolysis of plastic solid waste (PSW)," *J. Environ. Manage.*, vol. 197, pp. 177–198, Jul. 2017, doi: 10.1016/j.jenvman.2017.03.084.
[14] G. Zhang, Q. Mao, Y. Yue, R. Gao, Y. Duan, and H. Du, "Ni-based catalysts supported on Hbeta zeolite for the hydrocracking of waste polyolefins," *RSC Adv.*, vol. 14, no. 23, pp. 15856–15861, May 2024, doi: 10.1039/D4RA02809K.
[15] W. Luo *et al.*, "Catalytic Activity and Reusability of Nickel-Based Catalysts with Different Biochar Supports during Copyrolysis of Biomass and Plastic," *ACS Sustain. Chem. Eng.*, vol. 10, no. 30, pp. 9933–9945, Aug. 2022, doi: 10.1021/acssuschemeng.2c02392.
[16] H. Husin *et al.*, "Conversion of polypropylene-derived crude pyrolytic oils using hydrothermal autoclave reactor and ni/aceh natural zeolite as catalysts," *Heliyon*, vol. 9, no. 4, p. e14880, Apr. 2023, doi: 10.1016/j.heliyon.2023.e14880.
[17] B. Qu, T. Wang, X. Ji, T. Qin, Y. S. Zhang, and G. Ji, "Effect of reduction temperatures of Ni-modified zeolites on the product distribution, catalyst deactivation, and reaction mechanism during polypropylene pyrolysis," *Fuel*, vol. 384, p. 133947, Mar. 2025, doi: 10.1016/j.fuel.2024.133947.
[18] X. Hong *et al.*, "Hierarchical nitrogen-doped porous carbon with high surface area derived from endothelium corneum gigeriae galli for high-performance supercapacitor," *Electrochimica Acta*, vol. 130, pp. 464–469, Jun. 2014, doi: 10.1016/j.electacta.2014.03.015.
[19] M. C. Silva *et al.*, "H3PO4–activated carbon fibers of high surface area from banana tree pseudo-stem fibers: Adsorption studies of methylene blue dye in batch and fixed bed systems," *J. Mol. Liq.*, vol. 324, p. 114771, Feb. 2021, doi: 10.1016/j.molliq.2020.114771.
[20] F. Kurniawansyah, R. D. Pertiwi, M. Perdana, M. Al-Muttaqii, and A. Roesyadi, "Development of Bamboo - Derived Activated Carbon as Catalyst Support for Glucose Hydrogenation," *Mater. Sci. Forum*, vol. 988, pp. 108–113, Apr. 2020, doi: 10.4028/www.scientific.net/MSF.988.108.

[21] M. Iwanow, T. Gärtner, V. Sieber, and B. König, "Activated carbon as catalyst support: precursors, preparation, modification and characterization," *Beilstein J. Org. Chem.*, vol. 16, pp. 1188–1202, Jun. 2020, doi: 10.3762/bjoc.16.104.
[22] B. Qu, T. Wang, X. Ji, T. Qin, Y. S. Zhang, and G. Ji, "Effect of reduction temperatures of Ni-modified zeolites on the product distribution, catalyst deactivation, and reaction mechanism during polypropylene pyrolysis," *Fuel*, vol. 384, p. 133947, Mar. 2025, doi: 10.1016/j.fuel.2024.133947.
[23] X. Huang *et al.*, "Mechanistic Insights into Polypropylene Hydrogenolysis Using Ni/Al2O3 Catalysts," *Energy Fuels*, vol. 39, no. 3, pp. 1721–1734, Jan. 2025, doi: 10.1021/acs.energyfuels.4c04726.
[24] M. Thommes *et al.*, "Physisorption of gases, with special reference to the evaluation of surface area and pore size distribution (IUPAC Technical Report)," *Pure Appl. Chem.*, vol. 87, no. 9–10, pp. 1051–1069, Oct. 2015, doi: 10.1515/pac-2014-1117.
[25] K. S. W. Sing, "Reporting physisorption data for gas/solid systems with special reference to the determination of surface area and porosity (Recommendations 1984)," *Pure Appl. Chem.*, vol. 57, no. 4, pp. 603–619, Jan. 1985, doi: 10.1351/pac198557040603.
[26] L. Wu, Y. Li, Z. Fu, and B.-L. Su, "Hierarchically structured porous materials: synthesis strategies and applications in energy storage," *Natl. Sci. Rev.*, vol. 7, no. 11, pp. 1667–1701, Aug. 2020, doi: 10.1093/nsr/nwaa183.
[27] H.-S. Jeong and B.-J. Kim, "Effects of Nickel Impregnation on the Catalytic Removal of Nitric Oxide by Polyimide-Based Activated Carbon Fibers," *Nanomaterials*, vol. 13, no. 16, p. 2297, Aug. 2023, doi: 10.3390/nano13162297.
[28] Z. Refaat *et al.*, "Efficient CO2 methanation using nickel nanoparticles supported mesoporous carbon nitride catalysts," *Sci. Rep.*, vol. 13, no. 1, p. 4855, Mar. 2023, doi: 10.1038/s41598-023-31958-1.
[29] J. Du, A. Chen, S. Hou, and J. Guan, "CNT modified by mesoporous carbon anchored by Ni nanoparticles for CO2 electrochemical reduction," *Carbon Energy*, vol. 4, no. 6, pp. 1274–1284, 2022, doi: 10.1002/cey2.223.
[30] L. Jianming, Z. Jin, J. Shang, and Z. Jianguo, "Synergistic effect of porous carbon shell confinement and catalytic conversion of nickel nanoparticle cores for improved lithium–sulfur batteries," *RSC Adv.*, vol. 13, no. 19, pp. 12792–12798, 2023, doi: 10.1039/D3RA01339A.
[31] Q. Song, X. Yin, and H. Zhang, "Ni-MOF-74 Derived Carbon-Based Ni Catalysts for Efficient Catalytic Ammonia Synthesis via Pulsed DBD Plasma," *Plasma Process. Polym.*, vol. 22, no. 3, p. 2400173, 2025, doi: 10.1002/ppap.202400173.
[32] C. Jia *et al.*, "Highly Ordered Hierarchical Porous Single-Atom Fe Catalyst with Promoted Mass Transfer for Efficient Electroreduction of CO2," *Adv. Energy Mater.*, vol. 13, no. 37, p. 2302007, 2023, doi: 10.1002/aenm.202302007.
[33] A. I. Eldahshory, K. Emara, M. S. Abd-Elhady, and M. A. Ismail, "Catalytic pyrolysis of waste polypropylene using low-cost natural catalysts," *Sci. Rep.*, vol. 13, p. 11766, Jul. 2023, doi: 10.1038/s41598-023-37769-8.
[34] W. Cai *et al.*, "Catalytic pyrolysis of polypropylene waste for liquid fuels production using Ni/Al-MOF-derived catalysts," *Sustain.*, vol. 4, p. 100059, Jan. 2024, doi: 10.1016/j.nxsust.2024.100059.
[35] Y. Peng *et al.*, "A review on catalytic pyrolysis of plastic wastes to high-value products," *Energy Convers. Manag.*, vol. 254, p. 115243, Feb. 2022, doi: 10.1016/j.enconman.2022.115243.
[36] A. Fivga and I. Dimitriou, "Pyrolysis of plastic waste for production of heavy fuel substitute: A techno-economic assessment," *Energy*, vol. 149, no. C, pp. 865–874, 2018, doi: 10.1016/j.energy.2018.02.094.

[37] Q. Cheng *et al.*, "Degradation-catalysis of polypropylene into liquid fuel-range *iso*-olefins using Zn and Ni-incorporated microporous carbon," *J. Hazard. Mater.*, vol. 498, p. 139960, Oct. 2025, doi: 10.1016/j.jhazmat.2025.139960.